













Polysomnographic airflow shapes and site of collapse during drug-induced sleep endoscopy

Sara Op de Beeck ^{1,2,8}, Daniel Vena ^{3,8}, Dwayne Mann ⁴, Ali Azarbarzin ³, Phillip Huyett⁵,
Eli Van de Perck ¹, Laura K. Gell ³, Raichel M. Alex ³, Marijke Dieltjens ^{1,2}, Marc Willemen⁶,
Johan Verbraecken ^{6,7}, Andrew Wellman ³, Olivier M. Vanderveken ^{1,2,6} and Scott A. Sands ³

¹Translational Neurosciences, Faculty of Medicine and Health Sciences, University of Antwerp, Wilrijk, Belgium. ²Department of ENT, Head and Neck Surgery, Antwerp University Hospital, Edegem, Belgium. ³Division of Sleep and Circadian Disorders, Brigham and Women's Hospital and Harvard Medical School, Boston, MA, USA. ⁴School of Information Technology and Electrical Engineering, The University of Queensland, Brisbane, Australia. ⁵Department of Otolaryngology–Head and Neck Surgery, Massachusetts Eye and Ear and Harvard Medical School, Boston, MA, USA. ⁶Multidisciplinary Sleep Disorders Centre, Antwerp University Hospital, Edegem, Belgium. ⁷Laboratory of Experimental Medicine and Pediatrics (LEMP), Faculty of Medicine and Health Sciences, University of Antwerp, Wilrijk, Belgium. ⁸These authors contributed equally to this work.

Corresponding author: Sara Op de Beeck (Sara.opdebeeck@uantwerpen.be)



Shareable abstract (@ERSpublications)

This study provides a novel means to estimate site of pharyngeal collapse from clinical polysomnography, without drug-induced sleep endoscopy. Such information is needed to facilitate precise site-dependent treatments for obstructive sleep apnoea patients. <https://bit.ly/4ci9AHL>

Cite this article as: Op de Beeck S, Vena D, Mann D, *et al.* Polysomnographic airflow shapes and site of collapse during drug-induced sleep endoscopy. *Eur Respir J* 2024; 63: 2400261 [DOI: 10.1183/13993003.00261-2024].

Copyright ©The authors 2024.

This version is distributed under the terms of the Creative Commons Attribution Non-Commercial Licence 4.0. For commercial reproduction rights and permissions contact permissions@ersnet.org

This article has an editorial commentary:
<https://doi.org/10.1183/13993003.00767-2024>

Received: 1 June 2023
Accepted: 8 March 2024

Abstract

Background Differences in the pharyngeal site of collapse influence efficacy of non-continuous positive airway pressure therapies for obstructive sleep apnoea (OSA). Notably, complete concentric collapse at the level of the palate (CCCp) during drug-induced sleep endoscopy (DISE) is associated with reduced efficacy of hypoglossal nerve stimulation, but CCCp is currently not recognisable using polysomnography. Here we develop a means to estimate DISE-based site of collapse using overnight polysomnography.

Methods 182 OSA patients provided DISE and polysomnography data. Six polysomnographic flow shape characteristics (mean during hypopnoeas) were identified as candidate predictors of CCCp (primary outcome variable, $n=44/182$), including inspiratory skewness and inspiratory scoopiness. Multivariable logistic regression combined the six characteristics to predict clear presence ($n=22$) versus absence ($n=128$) of CCCp (partial collapse and concurrent tongue base collapse excluded). Odds ratios for actual CCCp between predicted subgroups were quantified after cross-validation. Secondary analyses examined complete lateral wall, tongue base or epiglottis collapse. External validation was performed on a separate dataset ($n_{\text{total}}=466$).

Results CCCp was characterised by greater scoopiness ($\beta=1.5\pm 0.6$ per 2SD, multivariable estimate \pm SE) and skewness ($\beta=11.4\pm 2.4$) compared with non-CCCp. The odds ratio for CCCp in predicted positive versus negative subgroups was 5.0 (95% CI 1.9–13.1). The same characteristics provided significant cross-validated prediction of lateral wall (OR 6.3, 95% CI 2.4–16.5), tongue base (OR 3.2, 95% CI 1.4–7.3) and epiglottis (OR 4.4, 95% CI 1.5–12.4) collapse. CCCp and lateral wall collapse shared similar characteristics (skewed, scoopy), diametrically opposed to tongue base and epiglottis collapse characteristics. External validation confirmed model prediction.

Conclusions The current study provides a means to recognise patients with likely CCCp or other DISE-based site of collapse categories using routine polysomnography. Since site of collapse influences therapeutic responses, polysomnographic airflow shape analysis could facilitate precision site-specific OSA interventions.

Introduction

Non-continuous positive airway pressure (non-CPAP) treatments for obstructive sleep apnoea (OSA) patients, including hypoglossal nerve stimulation and oral appliance treatment, are characterised by high adherence, yet their efficacy is patient-dependent [1]. An important determinant of suitability of these



therapies is the site, pattern and degree of pharyngeal collapse. Most notably, patients with complete concentric collapse at the level of the palate (CCCp) and/or oropharyngeal lateral wall collapse respond less favourably to hypoglossal nerve stimulation or oral appliance therapy than those with tongue base obstruction [2–6], with CCCp being a formal exclusion parameter for hypoglossal nerve stimulation treatment. In clinical practice, this information can be garnered from an advanced procedure known as drug-induced sleep endoscopy (DISE) where pharyngeal collapse characteristics are assessed using a flexible nasopharyngoscope during sedation designed to mimic natural sleep [7, 8]. However, currently the sites of pharyngeal collapse are not discernible *via* routine polysomnography.

Accumulating evidence supports the notion that different sites of collapse produce recognisably different airflow shape profiles during flow limitation [9–12]. During natural sleep, GENTA *et al.* [11] showed that inspiratory scoopiness, or negative effort dependence (NED), is associated with the site of collapse. Breaths during tongue base collapse showed little scoopiness, palatal or lateral wall collapse had moderate scoopiness, while epiglottis collapse showed high scoopiness [11, 12]. Furthermore, epiglottis collapse has been associated with high jaggedness and an elevated discontinuity index [9], while palatal prolapse during natural sleep was associated with increased expiratory flow limitation [10]. To date, however, no large study has utilised polysomnography to identify the site of collapse measured separately *via* DISE.

The current study sought to evaluate whether airflow shapes observed in a routine polysomnographic study can provide insight into the likely pharyngeal structures contributing to collapse as seen during DISE. Specifically, we developed a predictive model to identify the site and pattern of collapse using a small number of airflow shape characteristics (supplementary figure E1). Given the clinical implications of having CCCp during DISE, we focused on recognising this specific DISE pattern. We also specifically tested the hypothesis that CCCp during DISE is associated with greater scoopiness on polysomnography.

Methods

Participants

The current study describes the development of a prediction model using a new retrospective cohort of 182 subjects (“DISEpsg”) from Antwerp University Hospital (Edegem, Belgium) whose clinical data were collected specifically for the current protocol. All 216 candidate adult patients who had DISE between 1 January 2018 and 12 February 2020 and moderate-to-severe OSA (apnoea–hypopnoea index (AHI) >15 events·h⁻¹) on baseline polysomnography within 2 years of the DISE date were identified; 174 had already provided consent that covered the current analysis and an additional eight individuals signed additional informed consent, providing a total of 182 participants who provided written informed consent for analysis. The current study was registered at ClinicalTrials.gov with identifier number NCT04753684. Patients underwent DISE as part of their standard clinical care. DISE was performed as indication for mandibular advancement device, hypoglossal nerve stimulation or other surgical OSA treatment.

Polysomnography protocol

Patients underwent in-lab polysomnography at Antwerp University Hospital as part of routine clinical care (BrainLab RT; Natus Group (OSG), Kontich, Belgium). Patients were fitted with the standard polysomnography equipment including electroencephalography (six leads: F4, C3, C4, O1, M1 and M2), electrooculography, nasal pressure airflow (raw unfiltered), oximetry, breathing effort using respiratory induction plethysmography, body position and muscle activity. Pseudonymised data were exported to EDF file format and analysed using MATLAB 2018a (MathWorks, Natick, MA, USA). Hypopnoeas were scored according to the American Academy of Sleep Medicine 2012 guidelines [13, 14].

DISE protocol

DISE was performed by an experienced ear, nose and throat (ENT) surgeon, independent from the polysomnography measurement. Midazolam sedation (1.5 mg bolus) was maintained using target-controlled propofol infusion (2.0–3.0 µg). A flexible fiberoptic nasopharyngoscope (Olympus END-GP, 3.7 mm diameter; Olympus Europe, Hamburg, Germany) facilitated pharyngeal visualisation. The sites (palate, oropharynx, tongue base, hypopharynx, epiglottis), pattern (anteroposterior, concentric, laterolateral) and degree (partial, complete) of collapse were documented using a standardised scoring system [15]. To minimise inter-rater variability, data were scored prior to (and independently of) polysomnographic flow shape analyses by one ENT surgeon experienced in DISE (E. Van de Perck). For the current analysis, oropharyngeal and hypopharyngeal collapse categories were pooled to describe lateral wall collapse.

Our primary focus was to develop a prediction model with distinct flow shape characteristics that differentiates patients with CCCp (n=44) *versus* without CCCp. Accordingly: 1) patients with partial

concentric collapse were excluded from the primary analysis (n=10 for concentric palate) to reduce ambiguity relating to the presence of CCCp and 2) patients with concomitant CCCp and (complete or partial) tongue base collapse were removed (n=22), since a major goal was to discriminate between CCCp and tongue base collapse thereby initially avoiding complexities relating to multi-level collapse. Notably, we did not exclude lateral wall collapse from CCCp on the basis that they commonly occur together and CCCp may have overlapping lateral wall involvement. The impact of these decisions was carefully examined (see “Assessment of partial collapse” and “Assessment of multi-level collapse” in “Sensitivity analysis – alternative patient and sleep stage criteria” in the supplementary methods and results).

The secondary analyses examined complete lateral wall, tongue base and epiglottis collapse. For each analysis we also sought to minimise ambiguity; partial collapse categories were excluded. Where possible, multi-level collapse was minimised, *i.e.* for lateral wall collapse we excluded partial and complete tongue base collapse, for tongue base and epiglottis collapse we excluded complete lateral wall collapse and CCCp. See the Results for a summary of the individuals included in each analysis.

Data analysis overview

Our research strategy first involved visually reviewing flow shape characteristics during respiratory events of patients with CCCp *versus* without CCCp. Incorporating the knowledge gleaned from visual inspection, we manually selected a small number of interpretable flow shape characteristics and used these to develop a regression-based prediction model that identified patients at greatest odds of exhibiting CCCp as observed during DISE.

Flow shape characteristics

Flow shape calculation and model prediction are fully automated and rely minimally on human input. Feature selection that was part of model development was based on a combination of manual (visual) selection, expert opinion and statistical methods. Flow shape characteristics [16] describing aspects of non-rounded airflow behaviour (flattening, scooping, fluttering, within-breath timing features) were automatically calculated, six of which were selected in two phases.

In the first phase, we selected 25 characteristics using a bivariate screening procedure (see “Flow shape characteristics” in the supplementary methods for the complete list). In the second phase, using manual selection, six individual characteristics (table 1) were judiciously selected by investigators based on multiple approaches. First, high-frequency characteristics (snoring, flutter) were excluded because filtering can attenuate snoring in clinical practice. Second, visual inspection of the raw signals of the characteristic hypopnoea events (figure 1; see “Visualisation of characteristic events” in the supplementary methods) was used to visually compare patients with CCCp *versus* without CCCp; flow shape characteristics had to be interpretable and recognisably different in visual analysis. Likewise, characteristics relating to “scoopiness” (*i.e.* NED) were prioritised based on prior expectation [11]. Conceptually similar characteristics were avoided (*e.g.* flatness at different thresholds, multiple definitions of scoopiness/NED). Note, while flow shape characteristics of all individual breaths during hypopnoea were used for model development and during all other steps of feature selection, average flow shapes were constructed for visual inspection. Bivariate analysis results (CCCp *versus* non-CCCp) were also considered. Six characteristics were considered optimal and manageable from the perspective of future translational application and

TABLE 1 Shortlist of features that were included in the final analysis

Feature	Description
Scoopiness (negative effort dependence)	Lowest value of middle third of inspiration/highest value of last third of inspiration.
Inspiratory skewness	Skewness of the inspiratory flow shape. The time series of the inspiratory flow signal is treated as if it is a distribution of samples. A left-leaning breath is characterised by a greater inspiratory flow earlier in the breath.
Early inspiratory volume	Inspiratory volume at 30% of inspiratory duration.
Rise time	Time to 50% peak inspiratory flow/inspiratory duration.
Early inspiratory peak flow	Height of first peak/peak inspiratory flow.
Inspiratory peak time/ expiratory peak time	Time to peak inspiratory flow/time to peak expiratory flow.
A longlist of features is included in the supplementary methods.	

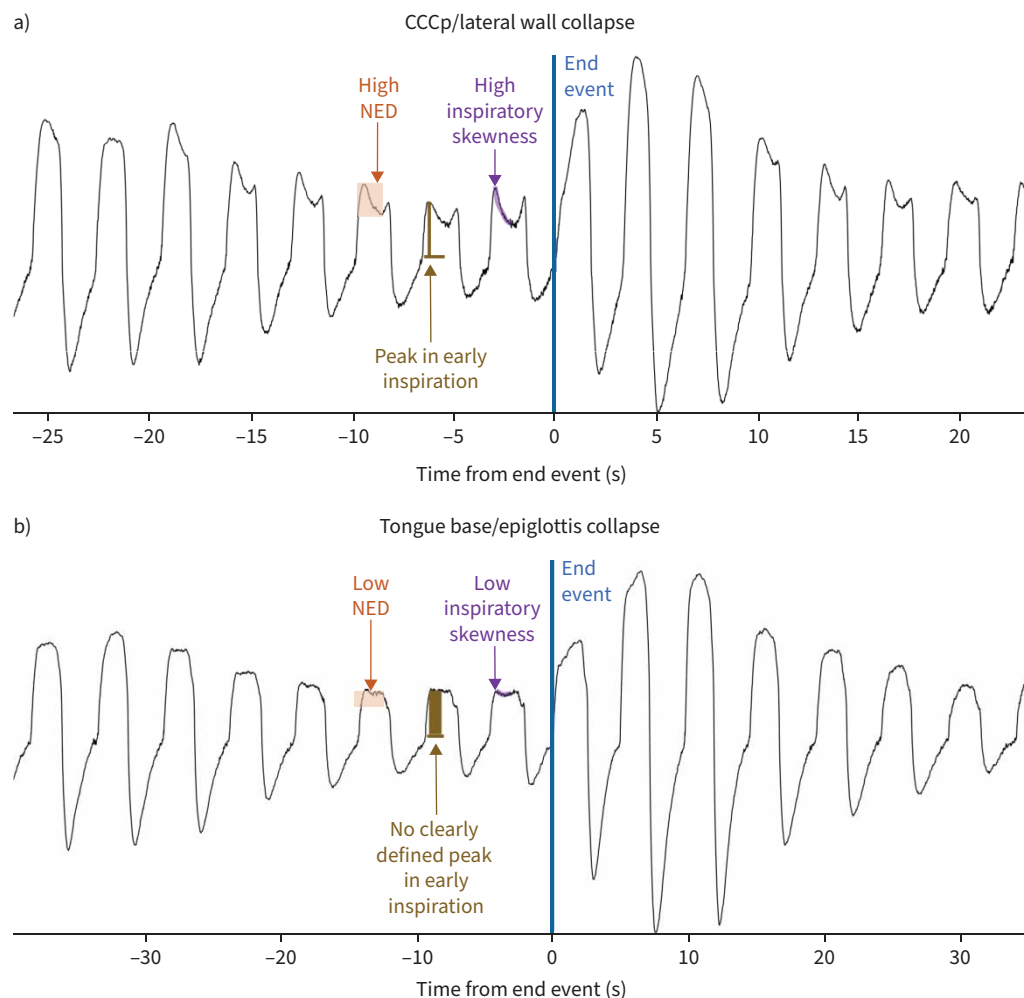


FIGURE 1 Visual inspection of characteristic event (ensemble average flow shape) for a) a representative patient with complete concentric collapse at the level of the palate (CCCp) and b) a patient with tongue base collapse. Patients with CCCp (a) exhibited increased scoopiness (higher negative effort dependence (NED)), increased inspiratory skewness (left-leaning inspiration) and greater early inspiratory peak flow, as shown. Other parameters included in the analyses were rise time, early inspiratory *versus* expiratory peak time and early inspiratory volume. Ensemble average flow shapes were constructed by ensemble averaging 15 breaths, centred around the scored end of the hypopnoea. Start and end points of each inspiration and expiration of each last hypopnoea breath were determined. Next, inspiration and expiration were averaged and joined back together. This process was repeated for all 15 positions of the ensemble average flow shape. A detailed overview on this technique is presented in “Visualisation of characteristic events” in the supplementary methods.

troubleshooting (see “Sensitivity analysis – number of flow shape characteristics used” in the supplementary methods). The same six characteristics were maintained for the prediction of other sites.

For each patient, a table was constructed with one row per breath (breaths outside hypopnoeas were excluded) that described the value for each of the six flow shape characteristics; mean values for each characteristic provided a representative value for each patient for analysis (supplementary figure E1).

Statistical analysis

Statistical analysis was performed using MATLAB. Statistical significance was considered if $p < 0.05$.

Primary analysis: CCCp

Multivariable logistic regression modelling combined the six characteristics (continuous independent predictor variables) to predict site of collapse (binary dependent variable). Odds ratios for true CCCp

between predicted subgroups (predicted absence and presence of CCCp) were quantified before and after leave-one-patient-out cross-validation to assess model predictive value.

Lateral wall, tongue base and epiglottis collapse

The primary analysis was repeated for the other collapse types, and for the pooled model differentiating patients with CCCp and/or complete lateral wall collapse from patients with tongue base and/or epiglottis collapse.

Night-to-night repeatability

To assess night-to-night repeatability, model-predicted CCCp probability was examined in a separate study, in which 18 patients underwent a baseline and placebo drug study [17]; here, pneumotach airflow was available rather than nasal pressure. Intra-class correlation (absolute agreement method) was used to describe repeatability of individual flow shape characteristics and the resultant model-predicted site of collapse probabilities across the 2 nights.

External validation

For external validation, we calculated model-predicted CCCp probability (plus other sites) in a separate study (“DISEflow”, n=466) performed at Mass Eye and Ear (Boston, MA, USA), in which patients with diagnosed OSA (any severity) underwent simultaneous DISE with pneumotachograph airflow. Logistic regression evaluated the association between true CCCp (binary dependent variable) with model-predicted CCCp probability (independent variable); analyses were repeated for other sites (see “External validation” in the supplementary methods for more details).

Results

Data from all 182 patients were analysed (table 2). Per patient, 148±71 hypopnoea events were included in the analysis, with a total of 706±433 breaths recorded during these hypopnoea events. Regarding DISE subgroups, 44 patients exhibited CCCp, 54 exhibited complete lateral wall collapse, 58 exhibited complete tongue base collapse and 28 exhibited complete epiglottis collapse. After exclusion of partial collapse and concomitant tongue base collapse (for CCCp and lateral wall collapse prediction) the main analytic samples were: CCCp (n=22/150), lateral wall collapse (n=26/104), tongue base collapse (n=37/113) and epiglottis collapse (n=18/158). See table 3 for details.

Complete prediction models

Primary analysis: CCCp

In multivariable regression, CCCp was associated with all six characteristics, notably greater scoopiness ($\beta=6.92\pm1.44$ per 2SD; $p<0.0001$, as hypothesised), greater skewness ($\beta=11.40\pm2.43$ per 2SD; $p<0.0001$, *i.e.* positively skewed/left-leaning), greater early inspiratory peak flow ($\beta=2.20\pm0.64$ per 2SD; $p=0.0006$), greater rise time ($\beta=1.48\pm0.75$ per 2SD; $p=0.047$), lower early inspiratory volume ($\beta=-14.44\pm3.23$ per 2SD; $p<0.0001$) and lower inspiratory versus expiratory peak time ratio ($\beta=-1.50\pm0.56$ per 2SD; $p=0.0076$) compared with patients without CCCp (pseudo- $R^2=0.31$, model $p<0.0001$, cross-validated accuracy 0.73 ± 0.04) (table 4; see also supplementary results). Additional adjustment for covariates (AHI, body mass index (BMI) and sex) had minimal effect on these multivariable associations (table 4, CCCp column, likelihood ratio test: $p=1.7\times10^{-7}$

TABLE 2 Baseline clinical characteristics for all patients (n=182) and the patient subgroups based on collapse type

	Overall (n=182)	CCCp (n=44)	Tongue base (n=58)	Lateral wall (n=54)	Epiglottis (n=28)
AHI (events·h ⁻¹ sleep)	24.2 (17.6–32.8)	27.7 (22.8–40.1)	24.6 (17.4–32.6)	26.3 (18.7–45.4)	26.0 (17.3–36.8)
BMI (kg·m ⁻²)	27.8 (25.2–30.5)	28.9 (26.9–32.1)	27.8 (25.4–30.6)	28.4 (26.0–31.2)	28.7 (25.7–30.5)
Age (years)	51.3 (40.4–58.8)	47.3 (35.6–55.8)	55.2 (42.7–61.2)	50.2 (39.1–57.3)	51.6 (41.5–60.5)
Neck circumference (cm)	40 (38–42)	40.5 (39.0–42.8)	39 (35–40)	41.0 (39.0–43.3)	40.0 (39.5–43.0)
Epworth Sleepiness Scale	10 (6–14)	11.0 (7–14.8)	10 (4–13)	9.0 (6.8–12.3)	11 (7–16)
Sex (male/female)	146/36	40/4	38/20	46/8	25/3
OAH (events·h ⁻¹ sleep)	22.7 (17.1–30.7)	27.3 (20.9–36.5)	23.2 (16.1–30.7)	25.2 (18.2–42.8)	26.0 (17.1–34.3)
ODI (events·h ⁻¹ sleep)	15.4 (10.8–24.0)	19.9 (11.7–32.4)	15.7 (11.9–22.1)	22.5 (12.1–30.9)	17.8 (13.0–28.4)
Hypopnoea index (events·h ⁻¹ sleep)	19.8 (15.9–28.2)	23.8 (19.0–31.5)	18.9 (15.3–27.3)	23.3 (17.0–37.9)	22.2 (15.5–28.7)
Apnoea index (events·h ⁻¹ sleep)	2.3 (0.4–5.8)	3.1 (0.5–7.9)	3.5 (0.4–8.6)	3.0 (0.7–7.5)	3.7 (1.4–9.7)

Data are presented as median (interquartile range) or n. CCCp: complete concentric collapse at the level of the palate; AHI: apnoea–hypopnoea index; BMI: body mass index; OAH: obstructive apnoea–hypopnoea index; ODI: oxygen desaturation index.

TABLE 3 Overview of the subjects included for each analysis

	Total	Concentric palate			Lateral wall			Tongue base			Epiglottis		
		C	P	N	C	P	N	C	P	N	C	P	N
All patients	182	44	10	128	54	50	78	58	48	76	28	14	140
CCCp model													
CCCp	22	22	0	0	10	9	3	0	0	22	3	0	19
Non-CCCp	128	0	0	128	33	29	66	48	32	48	19	12	97
LW model													
LW	26	10	2	14	26	0	0	0	0	26	2	0	24
Non-LW	78	9	3	66	0	0	78	32	19	27	17	9	52
TB model													
TB	37	0	1	36	0	9	28	37	0	0	8	4	25
Non-TB	76	22	6	48	26	23	27	0	0	76	11	4	61
EG model													
EG	18	0	3	15	0	2	16	8	4	6	18	0	0
Non-EG	140	34	6	97	45	43	52	41	38	61	0	0	140
CCCp/LW versus TB/EG													
CCCp/LW	33	19	2	12	24	7	2	0	0	33	0	0	33
TB/EG	34	0	0	34	0	0	34	27	3	4	13	3	18

Data are presented as n. C: complete collapse; P: partial collapse; N: no collapse; CCCp: complete concentric collapse at the level of the palate; LW: lateral wall collapse; TB: tongue base collapse; EG: epiglottis collapse. Red shading describes exclusion criteria designed to provide distinct examples of CCCp versus non-CCCp (and other collapse patterns) for prediction model development.

versus covariates alone; see supplementary table E3 for adjusted p-values). The odds ratio for CCCp in predicted CCCp versus predicted non-CCCp was 5.0 (95% CI 1.9–13.1) after cross-validation (table 4). Example breaths highlighting how CCCp may be recognised from the flow signal are shown in figure 2. Figure 3a shows how key characteristics contribute to predicted CCCp versus non-CCCp.

Secondary analyses: lateral wall, tongue base and epiglottis collapse

Separate models using the same flow shape characteristics provided promising prediction of complete lateral wall (n=26/104; cross-validated OR 6.3, 95% CI 2.4–16.5), tongue base (n=37/113; OR 3.2, 95% CI 1.4–7.3) or epiglottis (n=18/158; OR 4.4, 95% CI 1.5–12.4) collapse. Characteristics between CCCp and lateral wall collapse were similar (scoopy, left-leaning), and diametrically opposed to tongue base and epiglottis characteristics (table 4 and figure 3b–d).

An exploratory model discriminated between CCCp or lateral wall versus tongue base or epiglottis collapse (n=33/34; OR 7.5, 95% CI 2.5–22.1; pseudo-R²=0.46) (table 4 and figure 3e).

Figures including model slices and detailed tables with unstandardised β -values and probability cut-offs for all six characteristics of all models are included in the supplementary material (supplementary tables E3–E12 and supplementary figures E2–E6).

Night-to-night repeatability analysis

In a separate sample (n=18, 2 nights ~1–4 weeks apart, median (interquartile range) AHI 52 (24–75) events·h⁻¹, BMI 31 (27–35) kg·m⁻², age 45 (35–51) years [17]), intra-class correlations (ICCs) were 0.75–0.90 for the six individual flow shape characteristics (figure 4a) and 0.71–0.81 for site of collapse probability scores (ICC 0.76 for CCCp) (figure 4b) (see supplementary table E14).

External validation

External validation on data from a separate centre (n=466, median (IQR) AHI 28 (19–43) events·h⁻¹, BMI 29 (27–32) kg·m⁻², age 57 (48–64) years) showed a significant association between true CCCp and model-predicted CCCp probability score (n_{case}:n_{control}=14:349; OR 4.0 (95% CI 1.3–12.0) per SD increase). For lateral wall (n_{case}:n_{control}=84:157), tongue base (n_{case}:n_{control}=157:131) and epiglottis (n_{case}:n_{control}=13:275) collapse, similar associations were replicated (OR 2.2 (95% CI 1.3–3.9), 2.4 (95% CI 1.4–4.0) and 6.7 (95% CI 2.5–18.0) per SD, respectively). See “External validation” in the supplementary results for more details.

TABLE 4 Model parameters, odds ratios and performance after cross-validation for each model.

	Standard deviation	CCCp	LW	TB	EG	CCCp/LW versus TB/EG
n_{site of interest}:n_{controls}		22:150	26:104	37:113	18:158	33:34
Model parameters						
Scoopiness (negative effort dependence)	0.12	6.92±1.44 (p=1.4×10 ⁻⁶)	5.24±1.57 (p=0.0008)	-4.14±1.28 (p=0.0012)	-5.13±1.28 (p=6.0×10 ⁻⁵)	10.31±2.77 (p=0.0002)
Inspiratory skewness	0.14	11.40±2.43 (p=2.8×10 ⁻⁶)	10.74±3.30 (p=0.0011)	-7.87±2.51 (p=0.0017)	-14.69±3.22 (p=5.2×10 ⁻⁶)	20.38±5.94 (p=0.0006)
Early inspiratory volume	0.04	-14.44±3.23 (p=7.7×10 ⁻⁶)	-10.45±3.80 (p=0.0060)	9.49±3.25 (p=0.0035)	13.30±3.68 (p=0.0003)	-22.21±6.86 (p=0.001)
Rise time	0.11	1.48±0.75 (p=0.047)	1.14±0.90 (p=0.21)	-1.69±0.82 (p=0.0379)	-2.60±0.84 (p=0.0018)	4.47±1.64 (p=0.007)
Early inspiratory peak flow	0.08	2.20±0.64 (p=0.0006)	1.01±0.72 (p=0.16)	-1.12±0.67 (p=0.096)	-0.99±0.60 (p=0.099)	2.70±1.19 (p=0.023)
Inspiratory peak time/expiratory peak time	0.99	-1.50±0.56 (p=0.0076)	0.07±0.63 (p=0.91)	0.22±0.56 (p=0.699)	0.72±0.55 (p=0.19)	-0.99±0.92 (p=0.28)
Odds ratios (95% CI)						
Before cross-validation		19.8 (5.5–71.5) (p=4×10 ⁻⁸)	9.7 (3.5–27.0) (p=6×10 ⁻⁶)	6.9 (2.9–16.6) (p=8×10 ⁻⁶)	39.7 (5.1–307.8) (p=1×10 ⁻⁷)	32.3 (7.7–134.6) (p=2×10 ⁻⁸)
After cross-validation [#]		5.0 (1.9–13.1) (p=9×10 ⁻⁴)	6.3 (2.4–16.5) (p=2×10 ⁻⁴)	3.2 (1.4–7.3) (p=0.0069)	4.4 (1.5–12.4) (p=0.0071)	7.5 (2.5–22.1) (p=2×10 ⁻⁴)
Including AHI, BMI and sex after cross-validation		5.1 (1.9–13.4) (p=0.00125)	6.3 (2.4–16.5) (p=2×10 ⁻⁴)	2.4 (1.1–5.4) (p=0.04)	3.8 (1.4–10.5) (p=0.014)	23.6 (6.3–87.5) (p=1×10 ⁻⁷)
Performance						
Sensitivity						
Value±SEM		0.64±0.10	0.65±0.09	0.57±0.08	0.67±0.11	0.70±0.08
Chance value		0.31	0.34	0.38	0.35	0.46
p-value		0.0016	0.0007	0.022	0.005	0.003
Specificity						
Value±SEM		0.74±0.04	0.77±0.05	0.71±0.05	0.69±0.04	0.76±0.07
Chance value		0.69	0.66	0.62	0.65	0.54
p-value		0.15	0.03	0.08	0.31	0.002
Accuracy						
Value±SEM		0.73±0.04	0.74±0.04	0.66±0.04	0.68±0.04	0.73±0.05
Chance value		0.63	0.58	0.54	0.61	0.50
p-value		0.009	0.0002	0.0059	0.055	2.0×10 ⁺⁵
Positive predictive value						
Value±SEM		0.30±0.07	0.49±0.08	0.49±0.08	0.21±0.05	0.74±0.08
Chance value		0.15	0.25	0.33	0.11	0.49
p-value		0.023	0.005	0.035	0.067	0.002
Negative predictive value						
Value±SEM		0.92±0.03	0.87±0.04	0.77±0.05	0.94±0.02	0.72±0.07
Chance value		0.85	0.75	0.67	0.87	0.51
p-value		0.0089	0.003	0.049	0.018	0.004

Data for the model parameters are presented as log odds of the site of interest, β±SE per 2SD change in flow shape characteristic; positive and negative β-values are differentiated by darker and lighter red shading to indicate the direction of each association, respectively. CCCp: complete concentric collapse at the level of the palate; LW: lateral wall collapse; TB: tongue base collapse; EG: epiglottis collapse. #: primary measure of success. Performance without cross-validation is depicted in the supplementary results. All flow shape characteristics are unitless. p<0.05 is indicated in bold for the model parameters.

Discussion

Overall, this study showed that airflow shapes observed in a routine polysomnographic study can provide insight into the likely pharyngeal structures contributing to collapse seen during DISE. As hypothesised, CCCp was characterised by breaths with increased scoopiness. Combining six flow shape characteristics identified a subgroup of patients with 5-fold higher odds of exhibiting CCCp. Flow shape characteristics remained associated with CCCp after adjusting for covariates (AHI, BMI (typically higher in CCCp [18]) plus sex), demonstrating their novel predictive value for site of collapse detection. Furthermore, when assessed in a separate cohort, flow shape characteristics and their predicted site of collapse were repeatable across nights, supporting the notion that these measures can be considered a “trait” and overcome an important prerequisite for future clinical application.

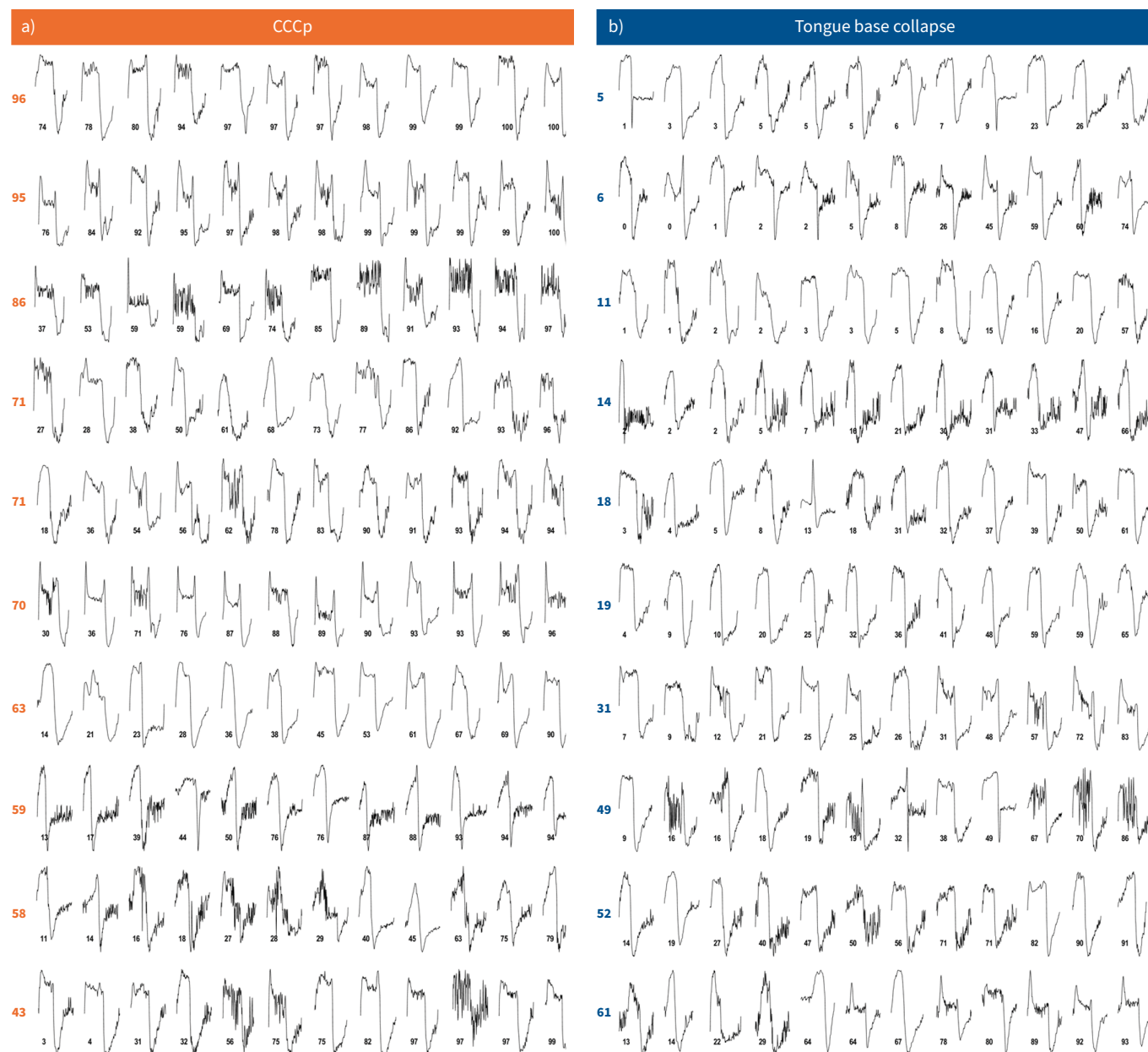


FIGURE 2 Raw individual breath data of a) patients with complete concentric collapse at the level of the palate (CCCp) and b) patients with tongue base collapse. Overall probabilities of CCCp or tongue base collapse per patient are depicted on the left-hand side of each panel. Probabilities of CCCp or tongue base collapse for individual breaths are depicted below each breath.

Novel physiological insight

Average flow shapes of patients with CCCp as measured during respiratory events (hypopnoeas) are characterised by increased scoopiness (NED), left-leaning inspiratory flow shapes and several additional features characterising similar behaviour, including faster inspiratory rise time, greater early peak flow (greater initial peak if multiple peaks are present) and a shorter time to peak inspiratory flow as a fraction of the time to peak expiratory flow. On the other hand, a reduced proportion of inspiratory tidal volume occurring in the first 30% of inspiratory time (lower “early inspiratory volume”) was independently predictive of CCCp, which we interpret as a form of calibration or reference for the aforementioned variables. The greater NED seen in CCCp in the current study is consistent with previous work demonstrating higher NED in breaths exhibiting “isolated palate” collapse compared with tongue base collapse (CCCp was not examined in this previous work [11]). Mechanistically, the increased NED seen in CCCp is likely to reflect a greater dynamic reduction and recovery of pharyngeal cross-sectional area

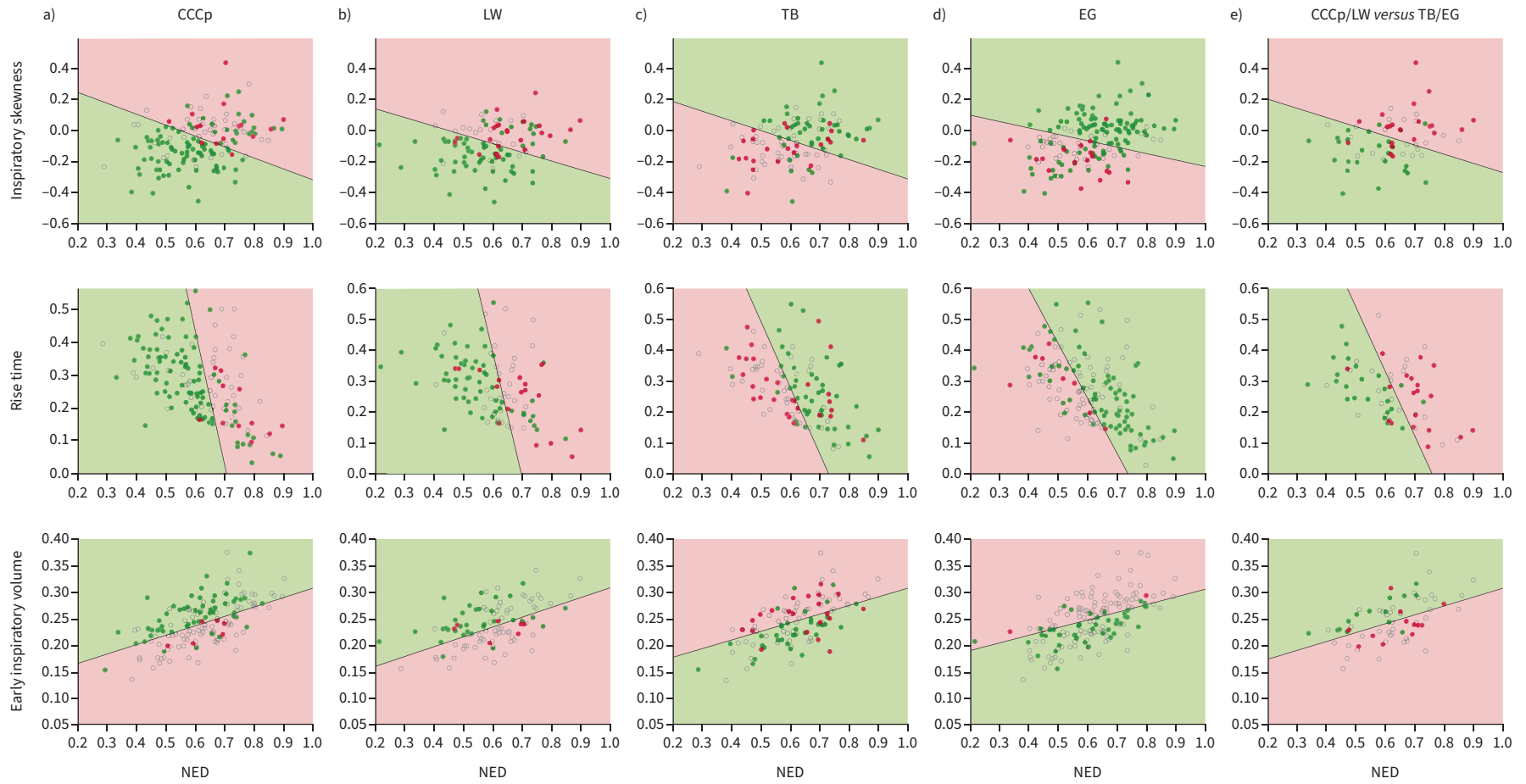


FIGURE 3 Simplified two-trait model “slices” for each of the five models: **a)** complete concentric collapse at the level of the palate (CCCp), **b)** lateral wall collapse (LW), **c)** tongue base collapse (TB), **d)** epiglottis collapse (EG) and **e)** CCCp/LW versus TB/EG. Each slice plot considers two of six features. The other four features in the model are at their mean value. Slices representing the most important model contributors (inspiratory skewness, rise time, early inspiratory volume and negative effort dependence (NED)) are depicted here. Full model representations are shown in the supplementary material. **a–d)** Patients with a certain collapse type are depicted in red, patients without this collapse type are depicted in green. Open circles denote patients for whom the model simplification does not apply as the other traits are too far from the mean value for this specific two-dimensional model “slice”. Background colours represent predicted presence of collapse. **e)** Green dots represent patients with TB or EG, red dots represent patients with CCCp or LW. Background colours depict the predicted site of collapse based on the model (green: TB or EG; red: CCCp or LW).

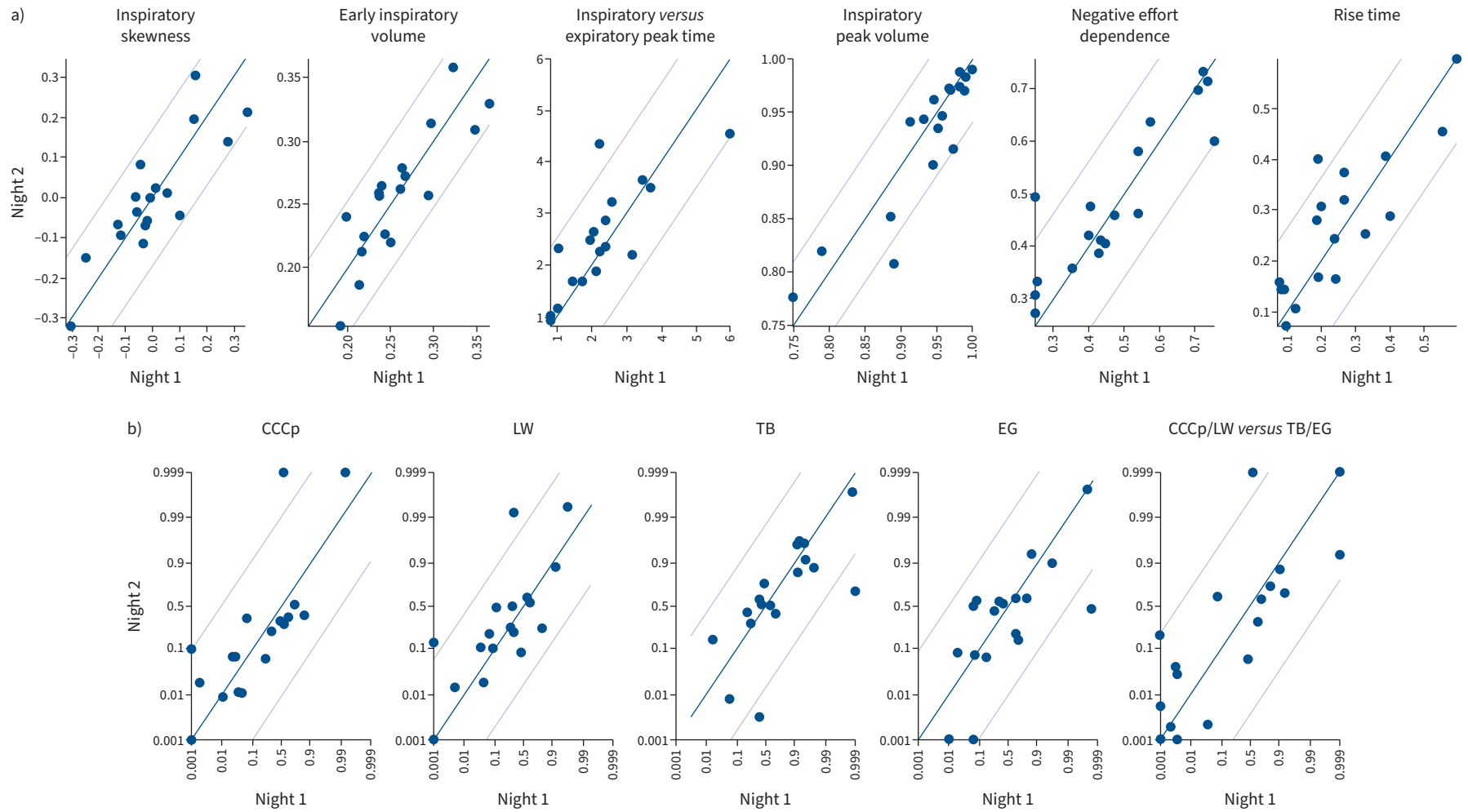


FIGURE 4 Repeatability analysis on a different cohort (n=18 subjects, n=36 total measurements), measured in a different centre. **a)** The six selected flow shape characteristics showed moderate to good reliability. **b)** Site of collapse prediction showed good reliability. CCCp: complete concentric collapse at the level of the palate; LW: lateral wall collapse; TB: tongue base collapse; EG: epiglottis collapse.

within inspiration, given the known association between NED and increased retropalatal compliance [19]. Along these lines, left-leaning breaths are considered to reflect a failure of the airway to respond to a meaningful within-breath increase in pharyngeal muscle activity; in principle, the typical ramp-like increase in pharyngeal muscle activity [20] should promote a gradual rise in inspiratory flow, resulting in right-leaning inspiratory shapes. Consistent with this interpretation, failure of CCCp to respond to increasing muscle activity is a known characteristic of this site/pattern of collapse [2, 21]. The mechanistic bases for the predictive value of the remaining characteristics are unclear.

The current study showed that, like CCCp, patients with lateral wall collapse also exhibited greater scoopiness and inspiratory skewness (left-leaning inspiration) during their respiratory events seen in conventional polysomnography. By contrast, tongue base collapse exhibited diametrically opposite characteristics compared with CCCp or lateral wall collapse (less scoopiness, right-leaning inspiration), consistent with the previous observation of lower NED in tongue base collapse *versus* other sites [11]. Here, epiglottis collapse characteristics overlapped substantially with tongue base collapse, with the addition of slower inspiratory rise time in epiglottis collapse. Less scoopiness, however, was unexpected given prior findings of greater scoopiness during epiglottis collapse [11, 12]; differences may lie with the use of averaged values here (all hypopnoea breaths) *versus* individual breath analysis previously [9, 11, 12]. We consider that epiglottis collapse is characteristically intermittent and/or non-sustained and may not always contribute to scored events [22]. A shared aetiology with tongue base collapse, however, is not unexpected: intuitively, a posteriorly located tongue may predispose to epiglottis collapse. These findings, taken together with the exploratory modelling (supplementary tables E14–E16 and supplementary figure E5), also suggested that the primary strength of flow shape characterisation is the ability to discriminate between CCCp/lateral wall collapse, located higher in the airway with a lateral component, and tongue base/epiglottis collapse, located lower in the airway with an anteroposterior component.

Clinical implications

Our study has clear clinical implications for patient selection for non-CPAP treatments, most of which are site-specific interventions. Specifically, CCCp and lateral wall collapse are associated with reduced efficacy of hypoglossal nerve stimulation [2, 6, 23] and mandibular advancement devices [4, 5], while tongue base collapse predicts favourable responses [3, 4]. Our finding that CCCp and lateral wall collapse appear distinct from tongue base collapse in flow shape characteristics therefore provides an avenue for mechanistically informed treatment selection. For example, patients interested in hypoglossal nerve stimulation could be counselled on their preference based on whether they have a high or low CCCp likelihood detected before proceeding with DISE. While preliminary work appears promising for treatment response prediction [24–26], further studies are needed to demonstrate clinical benefit.

Our study makes major steps towards translating the concept that flow shape characteristics differ between sites of collapse into clinical practice. Previous in-lab studies during natural and drug-induced sleep using simultaneous endoscopy and gold standard pneumotachograph flow associated the flow shape of manually selected individual breaths with its concurrent collapse type [9–12]. Here, we showed that automated analysis of the clinical airflow signal from a separate clinical polysomnogram contains the information necessary to predict CCCp likelihood (and other collapse sites, independent of known covariates AHI, BMI [18, 27] plus sex), such that advanced research-level signals data are not necessarily required. It is therefore highly feasible to estimate the probability of different sites of collapse without performing endoscopy.

Methodological considerations

We consider several limitations.

1) For model development, we opted to select patients with distinct presence *versus* absence of CCCp without the complicating influence of overlapping collapse sites, which involved the exclusion of multi-level collapse (CCCp plus tongue base). We considered whether including these patients could reduce the utility of flow shapes to predict CCCp. Additional analysis (supplementary figure E7) showed that a concurrent complete tongue base collapse masks CCCp to yield flow shape characteristics of non-CCCp. It might thus be difficult to predict CCCp with concomitant tongue base collapse. While this masking could be considered a limitation, tongue base collapse is associated with favourable outcome of several non-CPAP treatments [3, 4], such that the utility for response prediction may not be affected.

2) Model development was done on a rather small final sample size. However, validation of the results in a separate cohort from a different centre could be performed, highlighting the clinical utility of our findings.

3) We used averaged flow shape features to provide representative characteristics for each patient. While previous studies measured airflow with simultaneous endoscopy, the current study employed airflow and DISE data from separate studies. Thus, it was not possible to relate individual breaths to a specific collapse site. For epiglottis collapse in particular, expanding the analysis approach to individual breath-level analyses (e.g. “jaggedness”, “discontinuities” [9]) may allow for greater identification of epiglottis collapse in future.

4) Six flow shape characteristics were selected based on a combination of visual inspection and bivariate analysis with the goal of providing a simple interpretable model. It is possible that other selection techniques might have yielded stronger model performance; additional analyses were performed on each individual model to allow a) additional characteristics or b) replacement characteristics (see “Sensitivity analysis – number of flow shape characteristics used” in the supplementary methods). These models did not yield improvements in performance (cross-validated odds ratios).

5) DISE was used rather than natural sleep endoscopy for the labelled site of collapse, which may provide a source of additional uncertainty [28–30]. We might expect associations to be stronger if natural sleep was used. However, we emphasise that DISE is the current clinical standard used to characterise site of collapse and is known to provide insight into non-CPAP treatment efficacy [2–6, 31].

6) Night-to-night variability affects OSA severity [32] and may be expected to occur regarding flow shape classification. However, analysis of a separate cohort [17] showed good repeatability for individual flow shape characteristics and moderate to good repeatability for site of collapse prediction, suggesting that flow shape-based site of collapse provides a new trait that can be leveraged for better characterisation of the underlying causes of OSA in individual patients.

7) The site of pharyngeal collapse and its associated flow shape could be altered by sleep stage. In the current analysis, we opted to include all breaths during a hypopnoea event, regardless of sleep stage. Sensitivity analysis using only breaths during rapid eye movement (REM) or non-REM sleep suggests the developed model is driven by non-REM breaths (see “Sensitivity analysis – alternative patient and sleep stage criteria” in the supplementary methods and results). Further research is needed to allow evaluation of the site of collapse during REM sleep. The authors argue flow shape analysis could play an important role in this research, as flow shapes can be collected during REM sleep, which is impossible using the classic endoscopy techniques as sleep is too disturbed during natural sleep endoscopy, not allowing the patient’s sleep to progress to REM sleep and REM sleep is suppressed during DISE.

8) Finally, we demonstrated that polysomnographic flow shape characteristics could identify patients with increased odds of CCCp (OR ~5), yet accuracy was modest (73%). Although prediction certainty is not established on an individual level, the approach may help to identify a subgroup of patients for whom CCCp is particularly low likelihood (8% versus 30% in predicted non-CCCp) and thereby help move the field towards more precise clinical intervention.

Conclusions

Overall, the current study found that polysomnographic flow shape characteristics provide insight into CCCp likelihood as observed during a separate DISE procedure. Characteristics were similar between CCCp and lateral wall collapse, and distinctly different from tongue base and epiglottis collapse. By providing a means to predict site of collapse from a routine clinical study, our work has broad implications for the field’s goal of judicious provision of efficacious and tolerable therapies for a greater number of patients with OSA.

Ethics approval: All 216 candidate adult patients who had DISE between 1 January 2018 and 12 February 2020 and moderate-to-severe OSA on baseline polysomnography within 2 years of the DISE date were identified; 174 had already provided consent that covered the current analysis and an additional eight individuals signed additional informed consent, providing a total of 182 participants who provided written informed consent for analysis.

This study was registered at ClinicalTrials.gov with identifier number NCT04753684.

Author contributions: Conception and design of the work: S. Op de Beeck, D. Vena, A. Wellman, O.M. Vanderveken and S.A. Sands. Data collection/management: S. Op de Beeck, P. Huyett, E. Van de Perck, M. Dieltjens, M. Willems, J. Verbraecken and O.M. Vanderveken. Trait analysis and statistical analysis: S. Op de Beeck, D. Vena, D. Mann, A. Azarbarzin and S.A. Sands. Data interpretation: S. Op de Beeck, D. Vena, D. Mann and S.A. Sands.

Drafting the article: S. Op de Beeck, D. Vena and S.A. Sands. Critical revision of the article: all authors. Final approval of the version to be published: all authors.

Conflict of interest: S. Op de Beeck reports grants and travel support from Research Foundation Flanders (FWO). D. Vena receives personal fees as a consultant for Inspire Medical Systems. A. Azarbarzin receives personal fees as a consultant for Somnifix, ZOLL Respicaardia, Eli Lilly and Apnimed, and receives grant support from Somnifix, American Heart Association and American Academy of Sleep Medicine; in addition, A. Azarbarzin reports receipt of equipment from Philips Respironics, and the following patents: System and method for endo-phenotyping and risk stratifying obstructive sleep apnea, and Method, non-transitory computer readable medium and apparatus for arousal intensity scoring. P. Huyett is an education consultant for Inspire Medical Systems, and reports grants from Inspire Medical Systems and Nyxoah. J. Verbraecken reports grants and fees from SomnoMed, AstraZeneca, AirLiquide, Atos Medical, Vivisol, Mediq Tefa, Medidis, Micromed OSG, Bioprojet, Desitin, Epilog, Idorsia, Nightbalance, Inspire Medical Systems, Heinen and Löwenstein, Ectosense, Philips, ProSomnus, ResMed, Sefam, SD Worx, SOS Oxygène, Tilman, Total Care, Vlaamse Gemeenschap, Vlerick and ZOLL Itamar, and consultancy for Bioprojet, Idorsia and Epilog. A. Wellman works as a consultant for Apnimed, Somnifix, Inspire, Mosana, Takeda and Nox, and has received grants from the National Institutes of Health, Somnifix and Sanofi; in addition, A. Wellman has a financial interest in Apnimed, a company developing pharmacologic therapies for sleep apnoea, and holds a patent on flow shape analysis to detect the site of airway collapse. O.M. Vanderveken reports research support at Antwerp University Hospital outside the submitted work from ProSomnus, SomnoMed, Philips, Inspire Medical Systems, Nyxoah, Med-El and Cochlear, lecture honoraria from SomnoMed and Inspire Medical Systems, and consultancy for SomnoMed, Inspire Medical Systems and GlaxoSmithKline. S.A. Sands has served as a consultant for Apnimed, Nox Medical, Eli Lilly, Merck, LinguaFlex, Respicaardia, Forepoint and Inspire Medical, received grant support from Apnimed, ProSomnus, and Dynaflex, received royalties from the licensing of IP for pharmacological therapy for OSA, unrelated to the current study, lecture honoraria from Tufts University, and equipment from Nox Medical; his industry interactions are actively managed by his institution and has the following patents: Co-inventor on a patent for a combination pharmacological therapy therapy and Co-inventor on a patent OSA phenotyping using wearable technology. The remaining authors have not potential conflicts of interest to disclose.

Support statement: Sara Op de Beeck holds a Junior Postdoctoral Fellowship at Research Foundation Flanders (FWO) (1299822N) and acknowledges financial support for this publication by the Fulbright Visiting Scholar Program, which is sponsored by the US Department of State and the Commission for Educational Exchange between the USA, Belgium and Luxembourg. Its contents are solely the responsibility of the author and do not necessarily represent the official views of the Fulbright Program, the US Government or the Commission for Educational Exchange between the USA, Belgium and Luxembourg. D. Vena holds grants from the American Heart Association (938014) and the American Academy of Sleep Medicine (257-FP-21). D. Mann was supported by the University of Queensland (Research Stimulus Allocation Two, Fellowship) and the National Health and Medical Research Council of Australia (NHMRC 2001729, 2007001). M. Dieltjens holds a Senior Postdoctoral Fellowship at Research Foundation Flanders (FWO) (12H4516N). A. Azarbarzin reports grants from the American Heart Association and the American Academy of Sleep Medicine. A. Wellman reports grants from the National Institutes of Health (HL102321 and HL128658). O.M. Vanderveken holds a Senior Clinical Investigator Fellowship at Research Foundation Flanders (FWO) (1833517N). S.A. Sands was funded by the National Heart, Lung, and Blood Institute (R01 HL146697) and the American Academy of Sleep Medicine Foundation (228-SR-20). The funders were not involved in the study design, collection, the writing of this article or the decision to submit it for publication. Funding information for this article has been deposited with the Crossref Funder Registry.

References

- 1 Phillips CL, Grunstein RR, Darendeliler MA, *et al.* Health outcomes of continuous positive airway pressure versus oral appliance treatment for obstructive sleep apnea: a randomized controlled trial. *Am J Respir Crit Care Med* 2013; 187: 879–887.
- 2 Vanderveken OM, Maurer JT, Hohenhorst W, *et al.* Evaluation of drug-induced sleep endoscopy as a patient selection tool for implanted upper airway stimulation for obstructive sleep apnea. *J Clin Sleep Med* 2013; 9: 433–438.
- 3 Marques M, Genta PR, Azarbarzin A, *et al.* Structure and severity of pharyngeal obstruction determine oral appliance efficacy in sleep apnoea. *J Physiol* 2019; 597: 5399–5410.
- 4 Op de Beeck S, Dieltjens M, Verbruggen AE, *et al.* Phenotypic labelling using drug-induced sleep endoscopy improves patient selection for mandibular advancement device outcome: a prospective study. *J Clin Sleep Med* 2019; 15: 1089–1099.
- 5 Park P, Jeon HW, Han DH, *et al.* Therapeutic outcomes of mandibular advancement devices as an initial treatment modality for obstructive sleep apnea. *Medicine* 2016; 95: e5265.

- 6 Huyett P, Kent DT, D'Agostino MA, *et al.* Drug-induced sleep endoscopy and hypoglossal nerve stimulation outcomes: a multicenter cohort study. *Laryngoscope* 2021; 131: 1676–1682.
- 7 Croft CB, Pringle M. Sleep nasendoscopy: a technique of assessment in snoring and obstructive sleep apnoea. *Clin Otolaryngol Allied Sci* 1991; 16: 504–509.
- 8 De Vito A, Carrasco Llatas M, Ravesloot MJ, *et al.* European position paper on drug-induced sleep endoscopy: 2017 update. *Clin Otolaryngol* 2018; 43: 1541–1552.
- 9 Azarbarzin A, Marques M, Sands SA, *et al.* Predicting epiglottic collapse in patients with obstructive sleep apnoea. *Eur Respir J* 2017; 50: 1700345.
- 10 Azarbarzin A, Sands SA, Marques M, *et al.* Palatal prolapse as a signature of expiratory flow limitation and inspiratory palatal collapse in patients with obstructive sleep apnoea. *Eur Respir J* 2018; 51: 1701419.
- 11 Genta PR, Sands SA, Butler JP, *et al.* Airflow shape is associated with the pharyngeal structure causing OSA. *Chest* 2017; 152: 537–546.
- 12 Op de Beeck S, Van de Perck E, Vena D, *et al.* Flow-identified site of collapse during drug-induced sleep endoscopy: feasibility and preliminary results. *Chest* 2021; 159: 828–832.
- 13 Berry RB, Budhiraja R, Gottlieb DJ, *et al.* Rules for scoring respiratory events in sleep: update of the 2007 AASM Manual for the Scoring of Sleep and Associated Events. Deliberations of the Sleep Apnea Definitions Task Force of the American Academy of Sleep Medicine. *J Clin Sleep Med* 2012; 8: 597–619.
- 14 American Academy of Sleep Medicine Task Force. Sleep-related breathing disorders in adults: recommendations for syndrome definition and measurement techniques in clinical research. *Sleep* 1999; 22: 667–689.
- 15 Verbruggen AER, Vroegop AVMT, Dieltjens M, *et al.* Predicting therapeutic outcome of mandibular advancement device treatment in obstructive sleep apnoea (PROMAD): study design and baseline characteristics. *J Dental Sleep Med* 2016; 3: 119–138.
- 16 Mann DL, Terrill PI, Azarbarzin A, *et al.* Quantifying the magnitude of pharyngeal obstruction during sleep using airflow shape. *Eur Respir J* 2019; 54: 1802262.
- 17 Sands SA, Collet J, Gell LK, *et al.* Combination pharmacological therapy targeting multiple mechanisms of sleep apnoea: a randomised controlled cross-over trial. *Thorax* 2024; 79: 259–268.
- 18 Vroegop AV, Vanderveken OM, Boudewyns AN, *et al.* Drug-induced sleep endoscopy in sleep-disordered breathing: report on 1,249 cases. *Laryngoscope* 2014; 124: 797–802.
- 19 Marques M, Genta PR, Azarbarzin A, *et al.* Retropalatal and retroglottal airway compliance in patients with obstructive sleep apnea. *Respir Physiol Neurobiol* 2018; 258: 98–103.
- 20 Taranto-Montemurro L, Messineo L, Sands SA, *et al.* The combination of atomoxetine and oxybutynin greatly reduces obstructive sleep apnea severity. a randomized, placebo-controlled, double-blind crossover trial. *Am J Respir Crit Care Med* 2019; 199: 1267–1276.
- 21 Strollo PJ Jr, Soose RJ, Maurer JT, *et al.* Upper-airway stimulation for obstructive sleep apnea. *N Engl J Med* 2014; 370: 139–149.
- 22 Sung CM, Tan SN, Shin M-H, *et al.* The site of airway collapse in sleep apnea, its associations with disease severity and obesity, and implications for mechanical interventions. *Am J Respir Crit Care Med* 2021; 204: 103–106.
- 23 Dedhia RC, Huyett P. A prognostic star was born: drug-induced sleep endoscopy for hypoglossal nerve stimulation. *J Clin Sleep Med* 2020; 16: 15–16.
- 24 Vena D, Op de Beeck S, Mann D, *et al.* Pharyngeal site of collapse and collapsibility estimated from airflow predict oral appliance treatment efficacy. *Sleep Med* 2022; 100: S264–S265.
- 25 Vena D, Azarbarzin A, Marques M, *et al.* Predicting sleep apnea responses to oral appliance therapy using polysomnographic airflow. *Sleep* 2020; 43: zsa004.
- 26 Vena D, Huyett P, Op de Beeck S, *et al.* Flow-shape-derived site of pharyngeal collapse predicts response to hypoglossal nerve stimulation therapy. *Am J Respir Crit Care Med* 2023; 207: A6271.
- 27 Kastoer C, Benoist LBL, Dieltjens M, *et al.* Comparison of upper airway collapse patterns and its clinical significance: drug-induced sleep endoscopy in patients without obstructive sleep apnea, positional and non-positional obstructive sleep apnea. *Sleep Breath* 2018; 22: 939–948.
- 28 Van den Bossche K, Van de Perck E, Kazemeini E, *et al.* Natural sleep endoscopy in obstructive sleep apnea: a systematic review. *Sleep Med Rev* 2021; 60: 101534.
- 29 Park D, Kim JS, Heo SJ. Obstruction patterns during drug-induced sleep endoscopy vs natural sleep endoscopy in patients with obstructive sleep apnea. *JAMA Otolaryngol Head Neck Surg* 2019; 145: 730–734.
- 30 Ordonez AB, Grad GF, Cahali MB, *et al.* Comparison of upper airway obstruction during zolpidem-induced sleep and propofol-induced sleep in patients with obstructive sleep apnea: a pilot study. *J Clin Sleep Med* 2020; 16: 725–732.
- 31 Gogou ES, Psarras V, Giannakopoulos NN, *et al.* Drug-induced sleep endoscopy improves intervention efficacy among patients treated for obstructive sleep apnea with a mandibular advancement device. *Sleep Breath* 2022; 26: 1747–1758.
- 32 Sforza E, Roche F, Chapelle C, *et al.* Internight variability of apnea-hypopnea index in obstructive sleep apnea using ambulatory polysomnography. *Front Physiol* 2019; 10: 849.